Spectrochimica Acta Part A: Molecular and Biomolecular Spectroscopy 271 (2022) 120966

Contents lists available at ScienceDirect

Spectrochimica Acta Part A: Molecular and Biomolecular Spectroscopy

journal homepage: www.elsevier.com/locate/saa

Raman-based identification of tick species (*Ixodidae*) by spectroscopic analysis of their feces

Tianyi Dou [a], Alexei Ermolenkov [a], Samantha R. Hays [b], Brian T. Rich [b], Taylor G. Donaldson [b], Donald Thomas [d], Pete D. Teel [d], Dmitry Kurouski [a,c,*]

[a] Department of Biochemistry and Biophysics, Texas A&M University, College Station, TX 77843, United States
[b] Department of Entomology, Texas A&M AgriLife Research, College Station, TX 77843, United States
[c] Department of Biomedical Engineering, Texas A&M University, College Station, TX 77843, United States
[d] United States Department of Agriculture, Agricultural Research Service, Cattle Fever Tick Research Laboratory, 22675 North Moorefield Rd, Edinburg, TX 78541, United States

HIGHLIGHTS

- Raman spectroscopy (RS) and machine learning enable label-free, non-invasive and non-destructive identification of tick species via spectroscopic analysis of their feces.
- Spectroscopic signatures of feces are unique for different genera and species of ticks.
- RS can be used to predict the tick developmental stage and differentiate between nymphs, meta-nymphs and adult ticks.
- Timely detection of certain tick species on cattle can cease the spread of numerous devastating diseases such as Bovine babiesiosis and anaplasmosis.

GRAPHICAL ABSTRACT

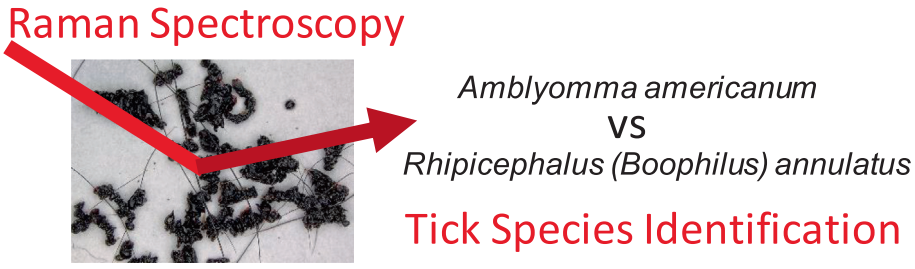

ARTICLE INFO

Article history:
Received 10 November 2021
Received in revised form 14 January 2022
Accepted 25 January 2022
Available online 29 January 2022

Keywords:
Confocal Raman spectroscopy
Hand-held Raman
Ixodidae Tick species differentiation
Tick feces
Partial least square discriminant analysis (PLS-DA)

ABSTRACT

Ticks are blood-feeding parasites that vector a large number of pathogens of medical and veterinary importance. There are strong connections between tick and pathogen species. Timely detection of certain tick species on cattle can cease the spread of numerous devastating diseases such as Bovine babiesiosis and anaplasmosis. Detection of ticks is currently performed by slow and laborious scout-based inspection of cattle. In this study, we investigated the possibility of identification of tick species (*Ixodidae*) based on spectroscopic signatures of their feces. We collected Raman spectra from individual grains of feces of seven different species of ticks. Our results show that Raman spectroscopy (RS) allows for highly accurate (above 90%) differentiation between tick species. Furthermore, RS can be used to predict the tick developmental stage and differentiate between nymphs, meta-nymphs and adult ticks. We have also demonstrated that diagnostics of tick species present on cattle can be achieved using a hand-held Raman spectrometer. These findings show that RS can be used for non-invasive, non-destructive and confirmatory on-site analysis of tick species present on cattle.

* Corresponding author.
E-mail address: dkurouski@tamu.edu (D. Kurouski).

https://doi.org/10.1016/j.saa.2022.120966
1386-1425/

1. Introduction

Ticks are blood-feeding ectoparasites of vertebrate animals and vectors of numerous pathogens of medical and veterinary importance [1]. Collection and identification of ticks, including those removed from host animals, is an essential surveillance activity [2,3]. Surveillance activities can provide early detection of exotic ticks, rates of geographic spread of newly introduced ticks, and essential monitoring in eradication and control programs.

The U.S. Cattle Fever Tick Eradication Program relies upon the human physical inspection of cattle, known as a "scratch inspection", to determine the presence of two species, *Rhipicephalus (Boophilus) annulatus* and *R. (B.) microplus,* both vectors of pathogens causing bovine babesiosis [4,5]. Physical inspection of live cattle to detect and remove ticks for identification is difficult and success is influenced by several factors [4,5]. Ticks must be of sufficient size (less than or equal to 8 mm in length) in their bloodfeeding to be detectable by human fingers. If the ticks are smaller, or if larger engorged ticks have dropped from the host at time of inspection, a false negative inspection may be determined. Ticks blood-feed for extended periods (days to weeks) and as blood is digested ticks defecate onto the host skin leaving a potential latent source of evidence and identification. Cattle may be infested with multiple tick species (family Ixodidae), including species in the genera *Amblyomma, Dermacentor*, and *Rhipicephalus*. These challenges catalyze a search for alternative approaches that can be used to detect and identify ticks on cattle.

Throughout the life cycle, ticks consume whole blood that consists of red and white blood cells, as well as platelets and plasma. Digestion involves midgut cell differentiation and intracellular digestion through endocytosis, elimination of waste and slow use of the resource for growth and reproduction [6]. Recent findings on enzyme biochemistry of several *Ixodidae* tick species suggests that variation in fecal chemistry may be species specific [7]. Expanding upon these findings, we hypothesize that detection and identification of tick species can be achieved via analysis of chemical composition of their feces.

Raman spectroscopy (RS) is an emerging technique that can be used to determine chemical composition of analyzed specimens [8]. This label-free, non-invasive and non-destructive analytical approach is based on a phenomenon of inelastic light scattering, which is taken place upon sample illumination with electromagnetic radiation. The inelastically-scattered photons provide information about the structure and composition of the analyzed specimens. RS is broadly used in various research areas ranging from forensics [9,10] and food processing [11] to agriculture [12–16] and electrochemistry [17]. For instance, Lednev group showed that animal species can be identified based on spectroscopic signatures of their blood [18]. This allows for a confirmatory differentiation between human and animal blood stains. Our own experimental findings show that RS can be used to identify plant species and their varieties, as well as diagnose biotic and abiotic stress in plants. A growing body of evidence suggests that RS can be used for diagnostics of human and animal diseases, such as cancer, Celiac and Lyme disease [19,20]. For instance, Farber and coworkers showed that chemical composition of mice blood drastically changes upon infection by *Borrelia burgdorferi*, bacteria that cause Lyme disease [21]. Changes in blood biochemistry can be detected by RS, which allows for confirmatory diagnostics of Lyme disease on different stages of bacterial infection.

In this study, we used RS to probe the structure and composition of feces of seven hard tick species found on cattle in south Texas, USA. Our results suggest that spectroscopic signatures of tick feces can be used for their confirmatory identification.

2. Materials and methods

Tick feces: Samples of tick feces were collected by brushing or scraping the dry hard pellets into clean glass vials from the skin of cattle used to feed ticks for maintenance of laboratory colonies. Vials were labeled for collection date, animal number, tick species and life stage, and stored at room temperature. Tick feces from *Amblyomma americanum, A. maculatum, A. mixtum, A. tenellum* and *Dermacentor albipictus* were collected from cattle used under IACUC approved Animal Use Protocol #2017-0345 at the Texas A&M AgriLife Tick Research Laboratory, College Station. Tick feces from *Rhipicephalus (Boophilus) annulatus* and *R. (B.) microplus* were obtained from cattle used under IACUC approved Animal Use Protocol 2017–0345 at USDA, ARS, Cattle Fever Tick Research Laboratory, Edinberg, Texas. Each tick species was being reared on separate animals, or in isolated feeding chambers ensuring fidelity of tick species to fecal sample source. During the rearing of the one-host ticks, *D. albipictus* and *R. (B.) annulatus*, fecal samples were collected during nymph and adult blood feeding to provide a source of comparison between developmental stages.

Raman spectroscopy: Raman spectra were collected on a home-built confocal microscope (Nikon TE-2000U). A single longitudinal diode mode laser (Necsel, CA, USA) was used to generate a continuous wavelength (CW) laser light (λ = 785 nm), which was focused on the sample using 20X Nikon objective (NA = 0.45). Scattered light was collected by the same objective and directed to a spectrograph (IsoPlane SCT 320, Princeton Instruments, NJ, USA) equipped with a 600 groove/mm grating blazed at 750 nm. Prior to entering the spectrograph Rayleigh scattering was filtered with LP02-785RE-25 long-pass filter (Semrock, NY, USA). The dispersed inelastically scattered photons were then captured by PIXIS:400BR CCD (Princeton Instruments, NJ, USA). A motorized stage H117P2TE (Prior, MA, USA) controlled by Prior Proscan II was used to move the tick fecal particles relative to the incident laser beam. All data were processed using GRAMS/AI 7.0 (Thermo Galactic, NH, USA).

Sample preparation: Particles of tick feces were selected from the sample collection depending on variation in color and texture (Fig. 1). Dark and white feces particles were included for *Amblyomma* and *Rhipicephalus* species. Dark particles were included for *Dermacentor albipictus* as these are the only variant produced. The spectra were collected from 20 to 25 different fecal particles for each species. Spectra acquisition time for *Amblyomma* and *Rhipicephalus* fecal particles was 10 s and for *D. albipictus* particles was 30 s.

Raman spectra shown in the Fig. 5 were collected using a handheld Resolve Agilent (Agilent, Santa Clara, CA, United States) spectrometer equipped with 830 nm laser source. The following experimental parameters were used for all the collected spectra: 1 s acquisition time, 495 mW power, and baseline spectral subtraction by device software.

Partial Least Square Discriminant Analysis: Partial Least Square Discriminant Analysis (PLS-DA) was used for statistical analysis of the collected Raman spectra. All the spectra were imported into MATLAB R2019a add-on PLS_Toolbox 8.6.2 (Eigenvector Research Inc.) The preprocessing method for all the spectra are area normalization and mean centering.

3. Results and discussion

3.1. Spectroscopic identification of tick species.

Raman spectra collected from feces of different tick species dominate with vibrational bands that can be assigned to guanine,

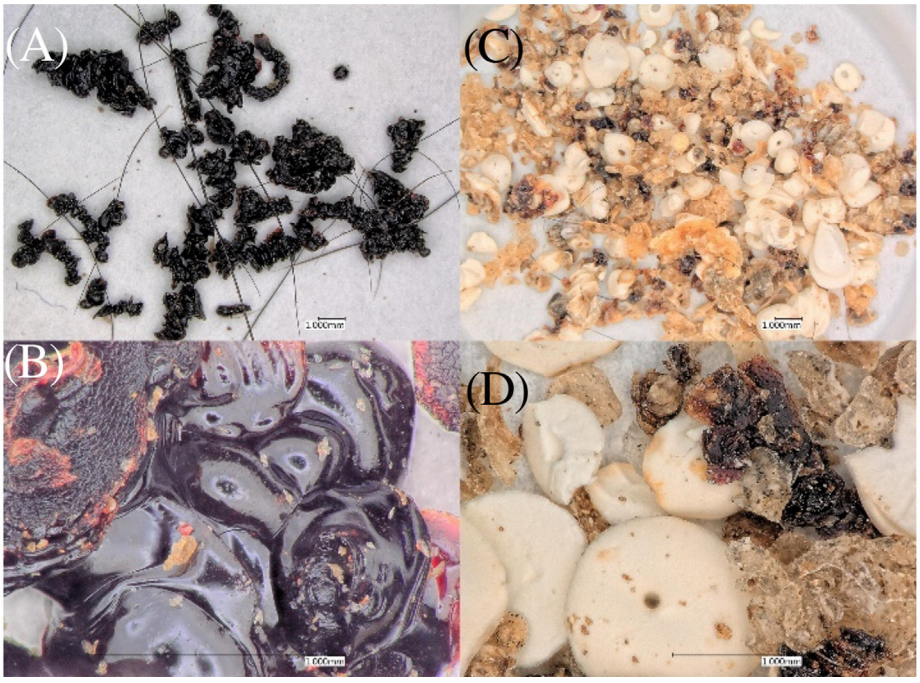

Fig. 1. Images of tick feces taken from the skin surface of cattle during colony maintenance rearing showing sample detail at 20X, and particle detail at 100X magnification for *Dermacentor albipictus*, A and B, and for *Amblyomma maculatum*, C and D, respectively.

the major chemical component of tick excrements, blood, collagen and keratin, Fig. 2 and Table 1. We also observed bands that are associated with vibrations of other nucleobases, such as uracil, adenine and cytosine [22,23]. In the collected spectra, we found several vibrational bands that could be assigned to various amino acids, such as alanine, serine, tryptophan, glutamate, cytosine, valine, threonine and glycine, as well as ascorbic acid, heme and lactose [19,21].

Raman spectra of *D. albipictus* and *R. (B.) annulatus* exhibit high similarities with previously reported spectra of blood [24]. These spectra have a distinct amide I band (1623–1643 cm^{-1}), as well as vibrational signatures of heme (1376, 1348 and 1162 cm^{-1}).

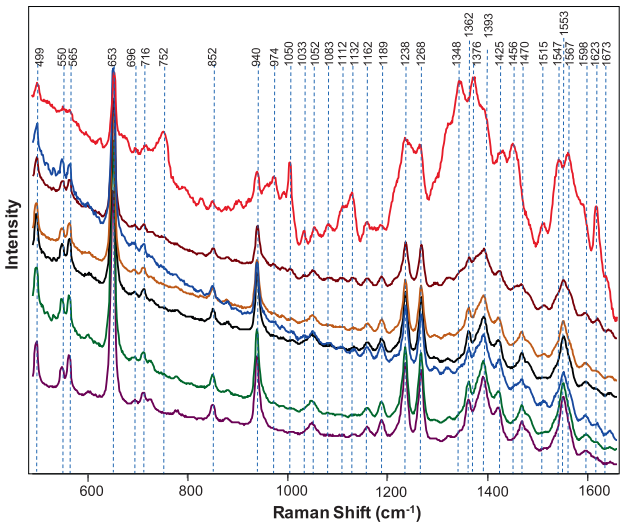

Fig. 2. Raman spectra of *Amblyomma americanum* (purple), *A. maculatum* (green), *A. tenellum* (blue), *A. mixtum* (black), *Rhipicephalus (Boophilus) microplus* (orange), *R. (B.) annulatus* (maroon) and *Dermacentor albipictus* (red). The spectra were averaged based on 20 to 25 spectra for each species.

We also observed vibrational bands at 1547, 1130, 1083 1008, 975, 905, and 755 cm^{-1} that have been previously reported for blood and could be assigned to aromatic and non-aromatic amino acids [25]. At the same time, spectra of *D. albipictus* and *(R.) (B.) annulatus* also exhibit vibrational bands that originate from guanine (Table 1). This indicates that feces of these tick species were composed of both blood and guanine. It should be noted that spectra of *D. albipictus* and *R. (B.) annulatus* have different relative intensities of blood and guanine vibrational bands, which allows for clear visual diagnostic of these two tick species based on their vibrational fingerprints. While spectra collected from feces of *D. albipictus* were nearly identical, Raman spectra acquired from *R. (B.) annulatus* could be divided into two classes, Fig. 3. One group of spectra exhibited predominantly blood-like vibrational fingerprint, whereas spectra from the second group were dominated by guanine bands. Raman spectra collected from *A. americanum, A. maculatum, A. tenellum, A. mixtum* and *R. (B.) microplus* appeared to have similar band patterns. Most of vibrational bands in these spectra could be assigned to guanine, Table 1. Although vibrational bands associated with blood were also present in these spectra, their intensities were substantially weaker compared to the intensities of corresponding bands in the spectra of *D. albipictus* and *R. (B.) annulatus*. It should be also noted that spectral variation within groups of *A. americanum, A. maculatum, A. tenellum, A. mixtum* and *R. (B.) microplus* was negligible.

Tick species (Ixodidae) identification can be achieved by comparison of relative intensities of bands in the reported spectra. However, one may note that such visual examination of band intensities is challenging. Therefore, we used multivariate statistical analysis to enhance diagnostic accuracy of tick species based on their Raman spectra. We conducted partial least-squares discriminant analysis (PLS-DA) to demonstrate that RS can be used for identification of ixodid tick species. First, we built the model that allows for differentiation between different genera of ixodid ticks, Table 2. The model enables 99.3%, 95.5% and 96.5% accurate prediction of *Amblyomma*, *Rhipicephalus (Boophilus)* and *Dermacentor* genera respectively.

Table 1
Vibrational bands and their assignments for the spectra collected from feces of seven different tick species.

Band (cm^{-1})	Assignment	Type
499	Guanine[25]	Ga/Gb/B
550	Cytosine[25], tryptophan[25], guanine[25]	Ga/Gb
565	Guanine[25], glycine[25], adenine[25], cytosine[25], thymine[25]	Ga/Gb
603	Cytosine[25], glycine[25], glutamate[25], phenylalanine[25]	Ga
653	Guanine[25]	Ga/Gb/B
696	Lactose[25], ascorbic acid[26]	Ga/Gb/B
715	Guanine[25]	Ga/Gb/B
727	Adenine[25], histdine[25]	Ga
752	Valine[25], tryptophan[25]	B
852	Guanine[25], tyrosine[27]	Ga/Gb
902	Valine[25]	B
940	Guanine[25]	Ga/Gb/B
974	Cytosine[25], histidine[25]	B
1006	Blood[21,27], collagen/keratin[28]	B
1033	Collagen/keratin[28]	B
1055	Guanine[25]	Ga/Gb/B
1083	blood[27]	Gb/B
1112	Alanine[25], histidine[25]	B
1132	Blood[27]	Gb/B
1162	Heme[27], guanine[25]	Ga/Gb/B
1189	Guanine[25]	Ga/Gb/B
1238	Guanine[25], collagen/keratin[28]	Ga/Gb/B
1268	Guanine[25]	Ga/Gb/B
1325	Serine[25], glycine[25]	Gb/B
1348	Heme[24]	B
1362	Guanine[25]	Ga/Gb
1376	Heme[21,27]	B
1392	Guanine[25]	Ga/Gb
1430	B-hematin[24]	Ga/B
1456	Collagen/keratin[28]	B
1470	Guanine[25]	Ga/Gb
1515	Valine[25]	B
1547	Guanine[25], blood[24]	Ga/Gb/B
1567	Heme[24]	B
1598	Glycine[25], alanine[25], serine[25]	Ga/Gb
1623	Blood[24]	Gb/B
1645	Blood[24], Collagen/keratin [28]	Gb
1673	Collagen/keratin[28], guanine[25]	Ga/B

Next, we built two PLS-DA models to differentiate species within genera *Amblyomma* and *Rhipicephalus (Boophilus)*. The prediction rates of the two models are all 100%, Tables 3 and 4. Our results demonstrate that coupling PLS-DA with RS, allows for a high (over 95%) accurate identification of tick species among those evaluated.

3.2. Spectroscopic identification of development stages of ticks

Measurements of *R. (B.) annulatus* feces collected at different time points of tick development (nymphs vs adults) are shown in Fig. 3. Our data demonstrate that tick feces excreted during nymph feeding of *R. (B.) annulatus* have more pronounced guanine-like signatures. At the same time, in the spectra collected from tick feces at late stages of tick development, heme-like signatures become more pronounced. These results suggest that spectroscopic signatures of tick feces may change depending on tick development stage.

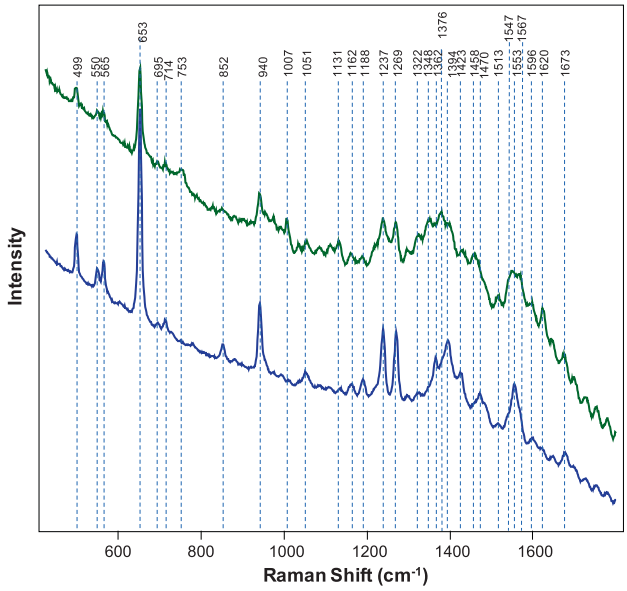

Fig. 3. Raman spectra taken from particles of *R. (B.) annulatus* feces that have predominantly blood-like (green) and guanine-like (blue) structures. The feces originate from the same group of ticks and were sampled one week apart from each other.

Table 2
Accuracy of classification by Partial Least Square Discriminant Analysis for Raman spectra collected from feces of three genera of ticks.

	Amblyomma	*Rhipicephalus (Boophilus)*	*Dermacentor*
Predicted as *Amblyomma*	447	0	0
Predicted as *Boophilus*	1	296	8
Predicted as *Dermacentor*	2	14	223
TPR (%)	99.3	95.5	96.5

For comparison, Fig. 4 summarizes spectra collected from feces excreted by feeding nymphs, by meta-nymphs during the intrastadial period and by feeding adults of *Dermacentor albipictus*.

Our results show that feces excreted by nymphs of *D. albipictus* have more heme-like composition, whereas the amount of guanine-like components increases as the species develops/molts to meta-nymph and adult stages. Specifically, we found that the band at 653 cm^{-1} increases as *D. albipictus* develops from nymph to adult. At the same time, intensity of the peak at 676 cm^{-1} continuously decreases. We have also observed a change in ratio of peaks at 939 and 977 cm^{-1}. In the spectra collected from nymph feces of *D. albipictus* the band at 977 cm^{-1} was found to be more intense than 939 cm^{-1}, whereas in the spectrum collected from adult feces of this tick species, we observed inversion of the peak intensities.

We built a PLS-DA model to enable accurate identification of different growth stages of *R. (B.) annulatus* and *D. albipictus* tick species, Tables 5 and 6 respectively.

Our data demonstrate that with 91% on average, RS can be used to predict whether the *R. (B.) annulatus* species present on the nymph or adult stages of development. Similar accuracy of prediction has been achieved for *D. albipictus*. Specifically, with 95.5%, 100% and 86.4% accuracy once can predict whether tick is present at nymph, meta-nymph or adult stages of development.

Table 3
Accuracy of classification by Partial Least Square Discriminant Analysis for Raman spectra collected from feces of four species of *Amblyomma* ticks.

	A. americanum	*A. maculatum*	*A. mixtum*	*A. tenellum*
Predicted as *A. ame*	142	0	0	0
Predicted as *A. mac*	0	97	0	0
Predicted as *A. mix*	0	0	165	0
Predicted as *A. ten*	0	0	0	46
TPR (%)	100	100	100	100

Table 4
Accuracy of classification by Partial Least Square Discriminant Analysis for Raman spectra collected from feces of two species of *Rhipicephalus* (*Boophilus)* ticks.

	R. (B.) annulatus	*R. (B.) microplus*
Predicted as *B. ann*	153	0
Predicted as *B. mic*	0	157
TPR (%)	100	100

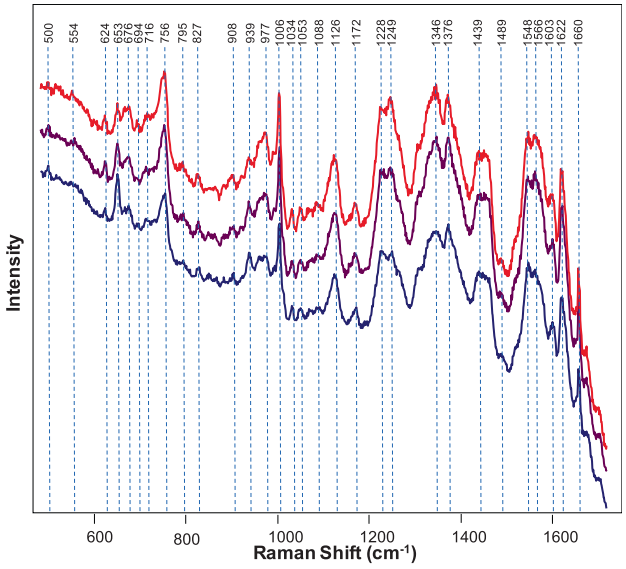

Fig. 4. Raman spectra taken from feces excreted by *Dermacentor albipictus* ticks feeding on cattle as nymphs (red), *meta*-nymphs (purple) and adults (blue).

These results demonstrate that metabolism of nymph and adult forms on the same tick species are different. In the case of *D. albipictus*, nymphs predominantly have heme-like excrements, whereas the amount of guanine component in adult feces increases. However, in the case of *R. (B.) annulatus* the order of these events in reversed. Nymphs of *R. (B.) annulatus* have guanine-like excrements, whereas adults of *R. (B.) annulatus* excrete predominantly heme-like compounds. Elucidation of detailed chemical composition of excrements is possible with the use of mass-spectroscopy. This work is beyond the scope of the current study.

3.3. Spectroscopic identification of tick species using a hand-held spectrometer

One may envision that practicality of such Raman-based diagnostics of ixodid tick species can be even further enhanced if tick species identification can be achieved by the use of a hand-held spectrometer. In the proof-of-principle experiment, we collected spectra from feces of two species: *A. americanum* (purple) and *A. maculatum* (green) using a hand-held Raman spectrometer. Our results show that excellent signal to noise in the collected spectra was achieved. It should be noted that spectral resolution of the hand-held spectrometer is 15 cm^{-1}, whereas spectral resolution of the confocal instrument is 2 cm^{-1}. Therefore, a peak doublet at 550–565 cm^{-1} could not be fully resolved on the hand-held spectrometer. Apart from that, all vibrational bands present in

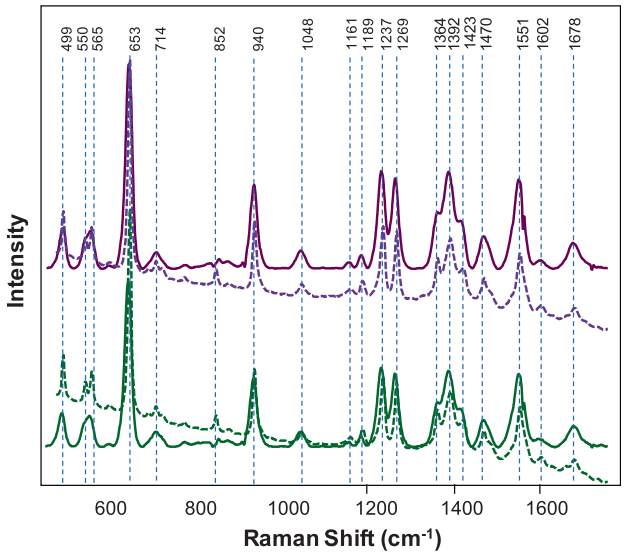

Fig. 5. Raman spectra taken from feces excreted by *Amblyomma americanum* (purple) and *A. maculatum* (green) using a hand-held Raman spectrometer (solid lines) and confocal spectrometer (dashed lines).

Table 5
Accuracy of classification by Partial Least Square Discriminant Analysis for Raman spectra collected from feces of *Rhipicephalus (Boophilus) annulatus* in two different growth stages.

	Nymph	Adult
Predicted as Nymph	40	5
Predicted as Adult	5	85
TPR (%)	88	94

Table 6
Accuracy of classification by Partial Least Square Discriminant Analysis for Raman spectra collected from feces of *Dermacentor albipictus* in three different growth stages.

	Nymph	Meta-nymph	Adult
Predicted as Nymph	21	0	3
Predicted as Meta-nymph	0	24	0
Predicted as Adult	1	0	19
TPR (%)	95.5	100	86.4

the spectra collected on a confocal Raman system were evident in the spectra collected using a hand-held spectrometer (Fig. 5).

The study of blood digestion in ticks has evolved from early morphological and physiological descriptions [8] of gut epithelium and digest cells to recent investigations of molecular and biochemical mechanisms of digestion [9]. These areas of investigation show both common features and differences in processes and systems between species in the two major tick families, *Ixodidae* and *Argasidae*, that support our findings of species-specific differences in tick feces identified by RS. Further, differences in fecal spectra between nymphal and adult stages of one-host ticks, may reflect different physiological and nutritional needs of adult ticks for mating and egg production, compared to needs during and between immature stages. Future studies will evaluate a wider array of tick species, further evaluate sample specificity and sensitivity, including mixed-species samples and the potential interference with other long-term blood-feeding ectoparasites (e.g., flies and lice) whose feces may confound identification.

4. Conclusion

In conclusion, we were able to show that RS can be used for confirmatory identification of tick species based on spectroscopic signatures of their feces using both confocal and hand-held Raman instruments. These findings support concepts for field applications of RS to identify tick infested animals. Finally, RS has provided insight into a new area of tick biology with potential field applications of surveillance and forensic value. These results resonate with the previously reported findings by our and other research groups which showed that RS could be used to probe changes in plant and animal metabolism [12,14,15,20,29]. These changes are specific to different biotic and abiotic stresses that life systems can experience. Consequently, laser-based detection of these changes can be used to detect and identified plant and animal diseases, including fungal, bacterial and viral infections.

CRediT authorship contribution statement

Tianyi Dou: Formal analysis, Investigation, Validation, Visualization. **Alexei Ermolenkov:** Formal analysis. **Samantha R. Hays:** Investigation, Validation, Visualization. **Brian T. Rich:** Investigation, Validation, Visualization. **Taylor G. Donaldson:** Investigation, Validation, Visualization. **Donald Thomas:** Investigation, Validation, Visualization. **Pete D. Teel:** Methodology, Writing – review & editing, Supervision. **Dmitry Kurouski:** Methodology, Writing – review & editing, Supervision.

Declaration of Competing Interest

The authors declare that they have no known competing financial interests or personal relationships that could have appeared to influence the work reported in this paper.

Acknowledgment

We are grateful for support provided in parts through the Texas A&M AgriLife Research Insect Vector Grants Program and through a USDA, APHIS, Cooperative Agreement M2100259. We also acknowledge support from the Governor's University Research Initiative (GURI) grant program of Texas A&M University, GURI Grant Agreement No. 12-2016, M1700437.

References

[1] F. Dantas-Torres, B.B. Chomel, D. Otranto, Ticks and tick-borne diseases: a One Health perspective, Trends Parasitol. 28 (10) (2012) 437–446, https://doi.org/10.1016/j.pt.2012.07.003.
[2] R.J. Eisen, C.D. Paddock, Tick and tickborne pathogen surveillance as a public health tool in the United States, J. Med. Entomol. 58 (4) (2021) 1490–1502, https://doi.org/10.1093/jme/tjaa087.
[3] A.T. Showler, A. Pérez de León, P. Saelao, Biosurveillance and Research Needs Involving Area-Wide Systematic Active Sampling to Enhance Integrated Cattle Fever Tick (Ixodida: Ixodidae) Eradication, J. Med. Entomol. 58 (4) (2021) 1601–1609, https://doi.org/10.1093/jme/tjab051.
[4] W.A. Palmer, N.L. Treverrow, G.H. O'Neill, Factors affecting the detection of infestations of Boophilus microplus in tick control programs, Aust. Vet. J. 52 (7) (1976) 321–324, https://doi.org/10.1111/j.1751-0813.1976.tb02397.x.
[5] P.D. Teel, M.S. Corson, W.E. Grant, M.T. Longnecker, Simulating biophysical and human factors that affect detection probability of cattle-fever ticks (Boophilus spp.) in semi-arid thornshrublands of South Texas, Ecol. Model. 170 (1) (2003) 29–43, https://doi.org/10.1016/j.ecolmodel.2003.05.002.
[6] S. Akov, Physiology of Ticks: Current Themes in Tropical Science, 1st edn., Pergamon Press, 1982.
[7] D. Sojka, Z. Franta, M. Horn, C.R. Caffrey, M. Mareš, P. Kopáček, New insights into the machinery of blood digestion by ticks, Trends Parasitol. 29 (6) (2013) 276–285, https://doi.org/10.1016/j.pt.2013.04.002.
[8] W.Z. Payne, D. Kurouski, Raman-based diagnostics of biotic and abiotic stresses in plants. A review, Front. Plant Sci. 11 (2021) 616672.
[9] K. Virkler, I.K. Lednev, Analysis of body fluids for forensic purposes: from laboratory testing to non-destructive rapid confirmatory identification at a crime scene, Forensic Sci. Int. 188 (1-3) (2009) 1–17.
[10] K. Virkler, I.K. Lednev, Blood Species Identification for Forensic Purposes Using Raman Spectroscopy Combined with Advanced Analytical Statistics, Anal. Chem. 81 (18) (2009) 7773–7777.
[11] M.R. Almeida, R.S. Alves, L.B. Nascimbem, R. Stephani, R.J. Poppi, L.F. de Oliveira, Determination of amylose content in starch using Raman spectroscopy and multivariate calibration analysis, Anal. Bioanal. Chem. 397 (7) (2010) 2693–2701, https://doi.org/10.1007/s00216-010-3566-2.
[12] C. Farber, D. Kurouski, Detection and identification of plant pathogens on maize kernels with a hand-held Raman spectrometer, Anal Chem 90 (5) (2018) 3009–3012, https://doi.org/10.1021/acs.analchem.8b0022210.1021/acs.analchem.8b00222.s001.
[13] L. Mandrile, S. Rotunno, L. Miozzi, A.M. Vaira, A.M. Giovannozzi, A.M. Rossi, E. Noris, Nondestructive Raman Spectroscopy as a Tool for Early Detection and Discrimination of the Infection of Tomato Plants by Two Economically Important Viruses, Anal. Chem. 91 (14) (2019) 9025–9031, https://doi.org/10.1021/acs.analchem.9b0132310.1021/acs.analchem.9b01323.s001.
[14] L. Sanchez, A. Ermolenkov, S. Biswas, E.M. Septiningshih, D. Kurouski, Raman Spectroscopy Enables Non-invasive and Confirmatory Diagnostics of Salinity Stresses, Nitrogen, Phosphorus, and Potassium Deficiencies in Rice, Front. Plant Sci. 11 (2020) 573321.
[15] L. Sanchez, S. Pant, M. Irey, K. Mandadi, D. Kurouski, Detection and Identification of Canker and Blight on Orange Trees Using a Hand-Held Raman Spectrometer, J. Raman Spectrosc. 50 (12) (2019) 1875–1880.
[16] S. Gupta, C.H. Huang, G.P. Singh, B.S. Park, N.-H. Chua, R.J. Ram, Portable Raman leaf-clip sensor for rapid detection of plant stress, Sci. Rep. 10 (2020) 20206.
[17] Z.C. Zeng, S. Hu, S.C. Huang, Y.J. Zhang, W.X. Zhao, J.F. Li, C. Jiang, B. Ren, Novel electrochemical Raman spectroscopy enabled by water immersion objective, Anal. Chem. 88 (19) (2016) 9381–9385, https://doi.org/10.1021/acs.analchem.6b02739.
[18] K.C. Doty, I.K. Lednev, Differentiation of human blood from animal blood using Raman spectroscopy: A survey of forensically relevant species, Forensic Sci. Int. 282 (2018) 204–210, https://doi.org/10.1016/j.forsciint.2017.11.033.
[19] N.M. Ralbovsky, I.K. Lednev, Towards development of a novel universal medical diagnostic method: Raman spectroscopy and machine learning, Chem. Soc. Rev. 49 (20) (2020) 7428–7453, https://doi.org/10.1039/d0cs01019g.
[20] N.M. Ralbovsky, I.K. Lednev, Analysis of individual red blood cells for Celiac disease diagnosis, Talanta 221 (2021) 121642, https://doi.org/10.1016/j.talanta.2020.121642.
[21] C. Farber, R. Morey, M. Krimmer, D. Kurouski, A.S. Rogovskyy, Exploring a possibility of using Raman spectroscopy for detection of Lyme disease, J. Biophotonics 14 (5) (2021), https://doi.org/10.1002/jbio.202000477e202000477.
[22] T.G. Burova, V.V. Ermolenkov, G.N. Ten, D.M. Kadrov, M.N. Nurlygaianova, V.I. Baranov, I.K. Lednev, Ionic and tautomeric composition of cytosine in aqueous solution: resonance and non-resonance Raman spectroscopy study, J. Phys. Chem. A 117 (48) (2013) 12734–12748, https://doi.org/10.1021/jp406228t.
[23] T.G. Burova, V.V. Ermolenkov, G.N. Ten, R.S. Shcherbakov, V.I. Baranov, I.K. Lednev, Raman spectroscopic study of the tautomeric composition of adenine in water, J. Phys. Chem. A 115 (38) (2011) 10600–10609, https://doi.org/10.1021/jp2033033.
[24] C.G. Atkins, K. Buckley, M.W. Blades, R.F.B. Turner, Raman Spectroscopy of Blood and Blood Components, Appl. Spectrosc. 71 (5) (2017) 767–793, https://doi.org/10.1177/0003702816686593.
[25] J. De Gelder, K. De Gussem, P. Vandenabeele, L. Moens, Reference database of Raman spectra of biological molecules, J. Raman Spectrosc. 38 (9) (2007) 1133–1147.

[26] J. Hvoslef, P. Klaeboe, B. Pettersson, S. Svensson, J. Koskikallio, S. Kachi, Vibrational Spectroscopic Studies of L-Ascorbic Acid and Sodium Ascorbate, Acta Chem. Scand. 25 (1971) 3043–3053, https://doi.org/10.3891/acta.chem.scand.25-3043.

[27] Y. Zou, P. Xia, F. Yang, F. Cao, K.e. Ma, Z. Mi, X. Huang, N. Cai, B. Jiang, X. Zhao, W. Liu, X. Chen, Whole blood and semen identification using mid-infrared and Raman spectrum analysis for forensic applications, Anal. Method. 8 (18) (2016) 3763–3767.

[28] M.C. Caraher, A. Sophocleous, J.R. Beattie, O. O'Driscoll, N.M. Cummins, O. Brennan, F.J. O'Brien, S.H. Ralston, S.E.J. Bell, M. Towler, A.I. Idris, Idris AI (2018) Raman spectroscopy predicts the link between claw keratin and bone collagen structure in a rodent model of oestrogen deficiency, Biochim. Biophys. Acta 1864 (2) (2018) 398–406, https://doi.org/10.1016/j.bbadis.2017.10.020.

[29] W.Z. Payne, T. Dou, J.M. Cason, C.E. Simpson, B. McCutchen, M.D. Burow, D. Kurouski, Non-Invasive Identification of Peanut Genotypes and Nematode Resistance Using Raman Spectroscopy, Front. Plant Sci. 12 (2021) 664243.